Sensors & Actuators: A. Physical 355 (2023) 114336

Contents lists available at ScienceDirect

Sensors and Actuators: A. Physical

journal homepage: www.journals.elsevier.com/sensors-and-actuators-a-physical

Self-powered photodetector array based on individual graphene electrode and silicon-on-insulator integration

Alper Yanilmaz [a,b,c], Özhan Ünverdi [d], Cem Çelebi [a,*]

[a] Quantum Device Laboratory, Department of Physics, Izmir Institute of Technology, Izmir 35430, Turkey
[b] Department of Photonics, Izmir Institute of Technology, Izmir 35430, Turkey
[c] Ermaksan Optoelectronic R&D Center, Bursa 16140, Turkey
[d] Faculty of Engineering, Department of Electrical and Electronic Engineering, Yasar University, Izmir 35100, Turkey

ARTICLE INFO

Keywords:
Graphene
Silicon-on-Insulator
Schottky junction
Photodiode Array
Optoelectronic Devices

ABSTRACT

One of the key limitations for the device performance of the silicon (Si) based photodetector arrays is the optical crosstalk effect encountered between photoactive elements as well. The scope of this work is to reduce optical crosstalk and thus increasing the device performances with graphene and Si integration. This paper presents the design, fabrication process, and performance evaluation of self-powered individual Graphene/Silicon on Insulator (GSOI) based Schottky barrier photodiode array (PDA) devices. A 4-element GSOI Schottky barrier PDA with *separate* graphene electrodes is fabricated to examine possible optical crosstalk encountered between each diode in the array structure. Here, monolayer graphene is utilized as hole collecting *separate* electrode on individually arrayed n-type Si on SOI substrate by photolithography technique. Each diode in the array exhibited a clear rectifying Schottky character. Photoresponse characterizations revealed that all diodes had excellent device performance even in self-powered mode in terms of an I_{light}/I_{dark} ratio up to 10^4, a responsivity of ~0.12 A/W, a specific detectivity of around 1.6×10^{12} Jones, and a response speed of ~1.32 μs at 660 nm wavelength. As revealed by optical crosstalk measurement, the device with pixel pitch of 1.5 mm had a total crosstalk of about 0.10% (−60 dB) per array. These results showed that the optical crosstalk between neighboring n-Si elements can be greatly minimized when graphene is used as separated electrode on arrayed Si on SOI substrate. Our study is expected give an insight into the performance characteristics of GSOI PDA devices which have great potential to be used in many technological applications such as multi-wavelength light measurement, level metering, high-speed photometry and position/motion detection.

1. Introduction

Silicon (Si) based p-n or p-i-n photodetector array (PDA) technologies have high demand due to their relatively high detectivity and response time in the field of high-value added technological applications such as motion and position detection [1], imaging [2], and spectrophotometry [3]. Si based photodetectors can arrange into Si units by stacking them one by one in a row but one of the substantial problem faced in such PDA is the optical crosstalk. Optical crosstalk includes the effect of photon refraction, reflection at boundaries, and external and internal scattering in detector arrays. As the photodiode size and the pitch (distance between photodiodes) of the detector array get smaller, there is a greater probability of crosstalk influencing system performance since the probability of a photogenerated carrier being collected by a neighboring junction increases. This situation causes the increment in the device noise, therefore, detection sensitivity of detector decreases accordingly. When the incident light on one element in PDA is coupled to neighbor one by reflection or by lateral diffusion of photogenerated charge carriers [4], optical crosstalk occurs due to the illumination technique and array geometry [5]. Apart from these, optical crosstalk can also appear with different doping concentration of the active junction layer [6] and can be controlled with the arranging the distance between the elements and the thickness of the device layer (i.e., absorption layer) [5] in different types of PDAs. In literature, there are lots of researches in the field of decrement in optical crosstalk effect of devices. In one study, Shirai et. al. [7] showed that optical crosstalk is minimized with the inclusion of trenches between adjacent channels for the 4 channel InGaAs-based vertical p-i-n photodiode array device. In

* Corresponding author.
E-mail address: cemcelebi@iyte.edu.tr (C. Çelebi).

https://doi.org/10.1016/j.sna.2023.114336
Received 17 January 2023; Received in revised form 9 March 2023; Accepted 26 March 2023
Available online 27 March 2023

another study, Menon et. al. [5] theoretically investigated that optical crosstalk can be decreased as distance between electrodes and the absorption layer thickness are increased for Si based interdigitated lateral p-i-n photodiode (ILPP) array devices. Besides the conventional fabrication routes for Si array packaging, it has been shown that silicon on insulator (SOI) structure enables well isolated Si units in a single substrate using standard microfabrication techniques, hence optical crosstalk between elements can be minimized using this technology [8]. Silicon-on-insulator (SOI) technology plays an important role to configure multiple photodiodes on single Si substrate. SOI structure consists of a thin single crystal Si film on amorphous buried oxide (SiO_2) layer (BOX) and handle Si, respectively. Here, BOX layer reduces leakage currents and provides full dielectric isolation between device and handle Si layers. This opportunity also improves the detection limits, and thus decreases the probability of the optical crosstalk between Si channels. Moreover, the use of SOI in the fabrication of PDA ensures remarkable advantages in regards to electrical leakage in sandwiched structure because the BOX also behaves as etch stop layer [8].

Self-powered photodetectors based on conventional semiconductor materials and 2D materials has been spotlighted in the field of energy-efficient applications due to its ease of fabrication, low noise ad relatively high bandwidth [9,10]. Especially, graphene/n-Si (G/n-Si) heterojunctions have been receiving a great deal of attention in the field of self-powered device applications due to outstanding device performances at room temperature [10]. In the last decade, it has been shown that Schottky junction can be easily constructed after transferring graphene onto n-type Si substrates benefiting from its planar structure [11, 12]. This construction generates the electric field arising from the built-in potential of ~ 0.5 – 0.7 V and separates the photo generated charge carriers at the depletion region of G/n-Si heterojunction even under a zero-bias regime [13,14]. The strong rectification between G/n-Si heterojunction enables the highly sensitive, self-powered and relatively fast photodetectors with respect to the p-n or p-i-n counterparts in the visible and short wavelength infrared spectral ranges [9].

Contrary to previous studies based on the fabrication of single pixel G/n-Si Schottky devices with different architectures [15–17], our previous work showed that monolayer graphene can be utilized as a *common* electrode on a lithographically defined as linearly four channel n-type Si arrays on a SOI substrate [18]. In order to further minimize the possible optical crosstalk between elements and hence decrease the dark current in junction, it has become important to separate and disconnected individual graphene electrodes on every single Si element in the array and examine the device performances. In literature, disconnected and separated graphene arrays can be patterned laterally on desired substrate using soft-patterning technique developed in Ref. [19] or inject printing method which represents performance and cost effectiveness in fabrication route. Recently, Grillo et. al. [20] showed that the four parallel graphene ink and Si heterojunction based diode arrays with Si *common* electrode can be manufactured on commercial heavily doped Si substrates using 'scratch and print' approach. In that study, Si is used as *common* electrode and the optical crosstalk between the diodes is inevitable due to the fact that photo-generation occurs mainly at the Si surface [21]. To the best of our experience, optical crosstalk problem can be eliminated in graphene and Si based PDA fabrication as following ways; (i) using graphene as *common* electrode, or (ii) individually patterning graphene electrodes on a single substrate using SOI technology. In this regard, we separated graphene electrodes by adding graphene patterning step on our previous work [18] and we successfully obtained individual graphene electrodes on arrayed Si channels and investigated the optoelectronic characteristics of each element. The scope of this work lies in the improvement of SOI based G/n-Si Schottky barrier PDAs with *separate* graphene electrode.

2. Experimental details

In this study, self-limiting growth of large area monolayer graphene was grown on 25 μm thick unpolished copper foil (99.8 purity, Alfa Aesar) cut into 10 × 10 mm^2 sized by Atmospheric Pressure Chemical Vapor Deposition (APCVD) method and transferred on desired substrate by means of the same procedure employed in our previous studies. [17, 22]. For the experiments, 10 μm thick n-doped photo-active silicon (Si (100)) and 10 × 10 mm^2 sized SOI substrates (specification ρ = 1–5 Ω. cm, nominal doping level $N_d \approx 2 \times 10^{15}$ cm^{-3}) were used. The device structures were prepared by using three-stage photolithography technique. An array of n-Si channels on SOI substrates was obtained by etching Si layer till the oxide layer (BOX) using Reactive Ion Etching (RIE) (Sentech Ins.) system. Graphene transfer was done using 'Photoresist (PR) Drop Casting' method. Firstly, Microposit S1318 PR as the supporting layer was dropped on the G/Cu and the stack was annealed at 70 °C overnight in an oven. The Cu foil at the bottom was fully etched using Iron Chloride ($FeCl_3$) solution to get suspended PR/G bilayer. After etching of possible $FeCl_3$ residues in H_2O: HCl (3:1) solution, the PR/G became ready for transfer process. As distinct from our previous work 'G/n-Si PDA with *common* graphene electrode' fabrication route [18], large area grown monolayer graphene was transferred on arrayed SOI substrate following the fabrication of Si array and shaped with thick photoresist (t~15 μm) using photolithography, subsequently graphene was etched with O_2 plasma to *separate* graphene electrodes. Following the graphene etching procedure, the windows for metal contact pads were defined by an additional lithography step on individually separated elements. After Cr (5 nm)/Au (80 nm) metals were evaporated both on the n-Si channel side and on the G/SiO_2 side of the SOI substrates with a thermal evaporator and then a lift-off process was applied to obtain individual one dimensional (1D) array device structure. A schematic illustration of the experimental process to fabricate the G/n-Si PDA device is displayed in Fig. 1. Finally, individual G/n-Si PDA on SOI with active junction area of 3 mm^2 become ready for optoelectronic measurements.

The electronic and optoelectronic characterizations of 4-Element G/n-Si Schottky PDAs were performed using tungsten-halogen lamp (Osram, 275 W) at room temperature under ambient conditions using a probe station interfaced with a power tunable monochromator light source (Newport, Oriel Cornerstone) including internal shutter, Keithley 2400 Source-Meter, Keithley 6485 Picoammeter, and a commercial Si photodiode FDS10×10 (Thorlabs). Time-resolved photocurrent measurements of the devices were evaluated for deep red wavelengths ranging employing 660 nm 1 W Power LED and function generator as LED driver with pulse modulation (Uni-t utg9005c). The photoresponse measurements of devices were acquired under 660 nm wavelength light pulsed with 1 kHz frequency and optical crosstalk measurements were taken using a 600 μm diameter fiber optic cable. The irradiation wavelength is specifically selected to be 660 nm since it corresponds to the maximum spectral response of our fabricated G/n-Si PDA on 10 μm thick SOI substrates.

3. Results and discussion

A cross-sectional view, schematic representation of the individually fabricated 4-element G/Si Schottky PDA and optical micrograph taken on diode is displayed in Fig. 2(a-c), respectively. After the transfer process, the quality and number of graphene layers on randomly selected spots on the diode surface was determined by single point Raman spectroscopy measurements. Raman signals were recorded in a spectral range between 1200 cm^{-1} and 3050 cm^{-1} using an Ar+ ion laser with a 532 nm excitation wavelength laser source was used with a 0.9 μm spot size. In all the measurements, graphene-related D, G, and 2D peaks were found at the peak wavelength of around ~1350, ~1602 and ~2685 cm^{-1}, respectively and well resolved as shown in Fig. 2(d). Strong G peak and weak D peak indicate good graphitic quality, and the

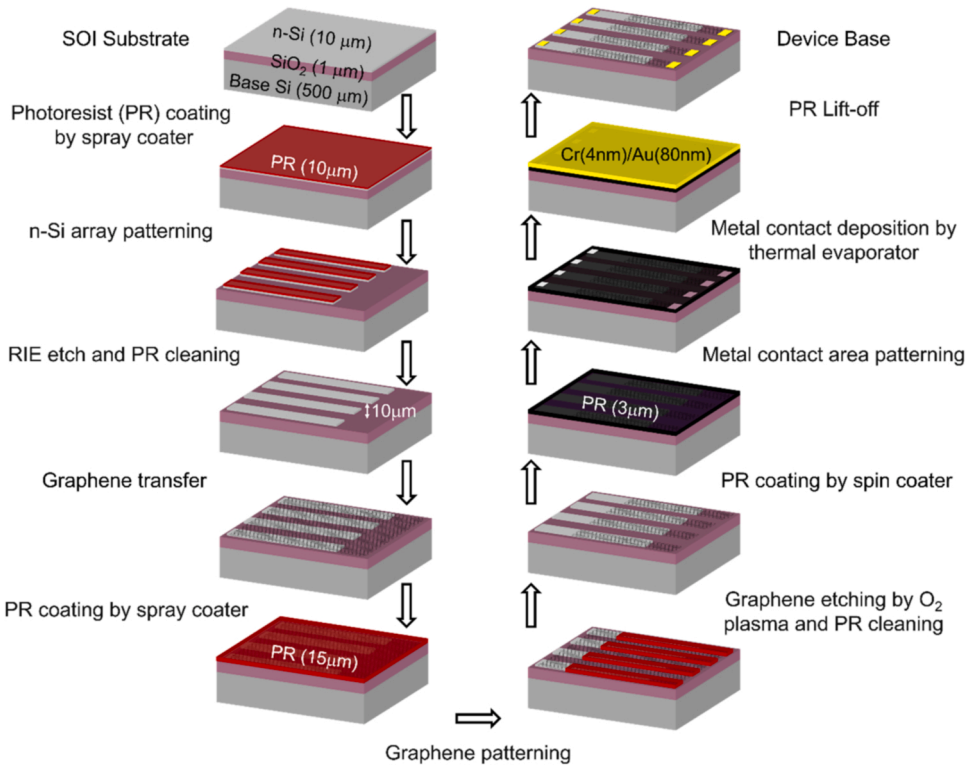

Fig. 1. Fabrication steps of 4-Element G/n-Si PDAs device base, followed by transferring and individually patterning graphene on SOI.

ratio of 2D peak intensity with G peak intensity ($I_{2D}/I_G > 2$) confirms that transferred CVD graphene is single layer on the device structure [23]. The active area where the graphene electrode making direct contact with the n-Si side was 3 mm^2. Prior to photocurrent spectroscopy measurements, the I–V measurements of each PD element on the SOI substrate with *separate* graphene electrode were conducted one by one under dark conditions with an applied bias voltage range between − 1 and 1 V. All the I-V curves of the diodes displayed typical rectifying Schottky contact behavior which is in good agreement with the thermionic-emission (TE) model [24] given as;

$$I = I_0\left[\exp\left(\frac{qV}{\eta kT}\right) - 1\right] \quad (1)$$

where I_0 is the reverse saturation current which is written as,

$$I_0 = AA^*T^2\exp\left(-\frac{q\Phi_B}{kT}\right) \quad (2)$$

where A is the junction area (0.03 cm^2), A* is the effective Richardson constant (112 A/cm^2K^2 for n-Si), T is the temperature (300 K), Φ_B is the Schottky barrier height, k is the Boltzmann constant, q is the elementary charge and η is the ideality factor. From the I–V plots, the dark current (I_d) and saturation current (I_0) values were determined were determined as ~0.4 nA and 2.61×10^{-8} A in average for PD elements, respectively. In the forward-bias range, although the current increases linearly at very small voltages, the deviation from linearity observed at relatively high voltages is due to the series resistance contributions from the underlying n-Si element. The slight difference seen at the reverse bias saturation currents suggests only a small variation in the rectification strength of the G/n-Si heterojunction. For a detailed comparison, the I–V data were plotted in the semi-logarithmic scale as shown in Fig. 2(e). Using the method developed by Cheung et al.[25], the average Schottky barrier height (Φ_B) and the ideality factor (η) of the PD elements with *separate* graphene electrode were extracted from the linear forward-bias region of the log(I)–V plot as ~0.81 eV and ~1.51, respectively. Considering the Schottky–Mott model, where Φ_B is defined as the difference between the work function of graphene (W_G) and the electron affinity of Si (χ_{Si} = 4.05 eV), W_G was calculated as ~4.86 eV in average for PD elements, respectively. These two diode parameters are consistent with our previous work [18] and those of G/n-Si based Schottky barrier photodiodes fabricated on thick n-Si substrates [26].

For optical crosstalk measurements, we used an LED source with 660 nm wavelength coupled to a fiber optic cable tip with 600 μm core diameter to locally illuminate each individual diodes and SiO_2 regions between them in the PDA. Each diode has a Si dimensions with length and width of 5 mm and 1 mm, respectively. The length between elements is kept constant as 1.5 mm (Fig. 3(a)). Firstly, an optical source is provided to only one pair of the anode (n-Si) – cathode (G) electrodes in the individually arrayed photodiodes where the separate cathode is biased with a certain voltage range between − 1 and 1 V. The distance between the sample and the tip of the fiber optic cable was kept at ~1 mm to ensure a well-defined spot size and avoid possible back reflections that may respectively arise from the illuminated Si surface and the metallic tip of the fiber optic probe used in the experiments. From the log(I)–V plot shown in Fig. 3(b), the short-circuit current (I_{SC}) where photocurrent measured at zero-bias were determined to be varying in a range between 4.2 and 7.5 μA. In the case when the light source is brought on the SiO_2 regions located in between two neighboring active elements, the zero-bias currents of diodes were measured as ~5 nA which is more than almost tenfold compared to the corresponding I_d values. As depicted in Fig. 3(a) with 4 pairs of electrodes, optical illumination is present on the junction of D2. Subsequently, the generated photocurrent at every other anode-cathode electrode pair (i.e. D1, D3, and D4) is extracted in the same measurement, respectively. The total crosstalk as amplitude in any array can be determined as the total sum of photocurrent at diode I_{Dn} (excluding the illuminated diode) over the photocurrent generated at the illuminated element and can be written as [5];

$$\text{Total Crosstalk} = 20 * \log\left(\frac{I_{D1} + I_{D3} + I_{D4}}{I_{D2}}\right) \quad (3)$$

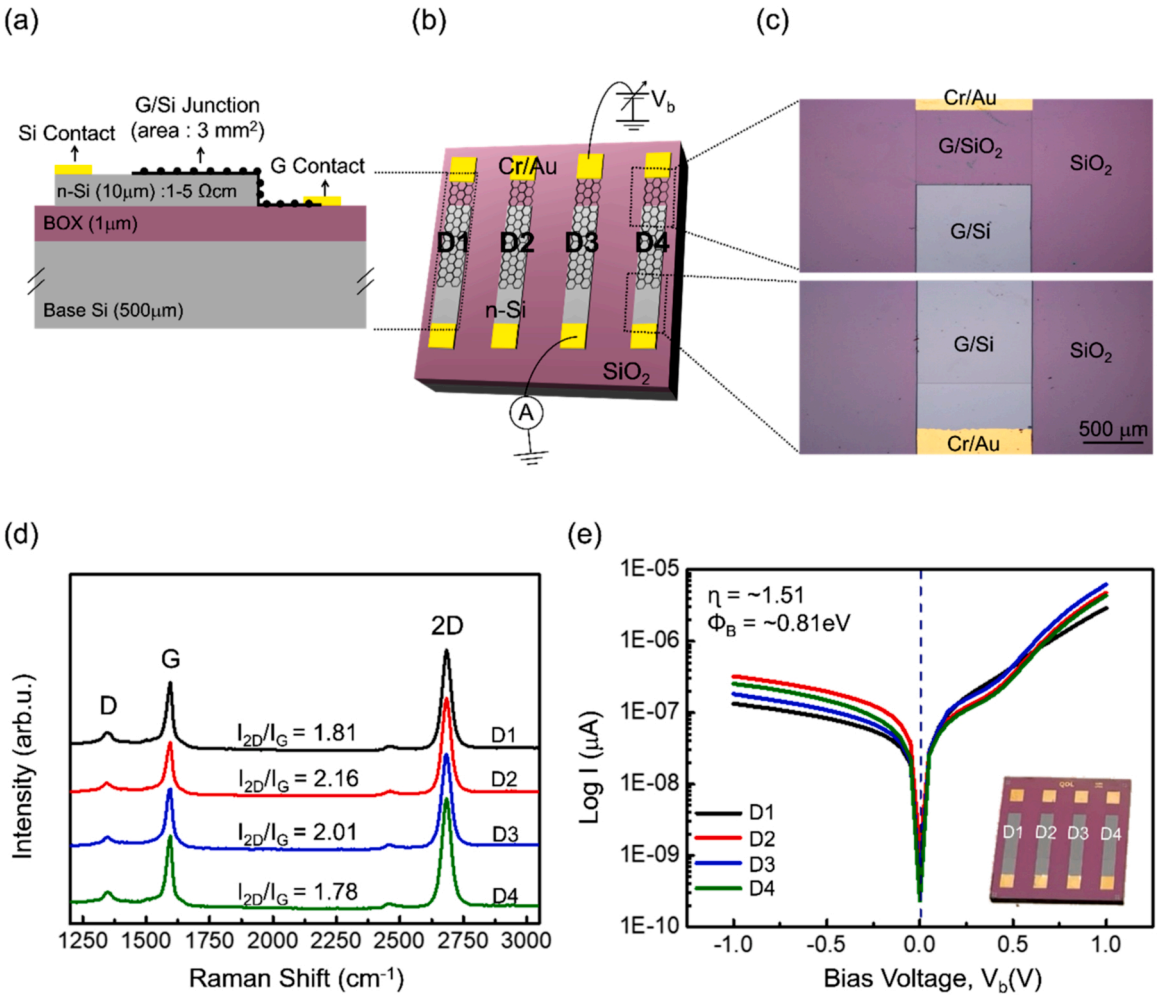

Fig. 2. (a) The cross-sectional view of the device where graphene is transferred on the planar Si (100) surface and (b) schematic structure of the fabricated individual G/n-Si PDA device (D1, D2, D3, and D4 represent the G/n-Si diodes arrayed on SOI), (c) optical micrograph of the diodes, (d) a typical single-point Raman spectrum taken on randomly selected region of the diodes and (e) the log(I)-V plot of the devices with separate graphene electrode in dark which was used to extract the η and Φ_B of each element. Inset: Device photograph.

where I_{Dn} is the photocurrent that flows at the anode indexed as n = 1,2,3,4 and I_{D2} is the measured photocurrent in diode D2. Therefore, when D2 is illuminated, the possible optical crosstalk at D1 can be calculated with [5]:

$$\text{Crosstalk} = 20 * \log\left(\frac{I_{D1}}{I_{D2}}\right) \quad (4)$$

This relation can be generalized to calculate other crosstalk values occurred in other elements. Using Eq. 4, under the illumination of D2 ($I_{SC(0\ V)} = 4.2$ μA), we calculated the crosstalk values of − 59 dB (0.11%), − 57 dB (0.14%) and − 60 dB (0.10%) at D1 ($I_{(0\ V)} = 5$ nA), D3 ($I_{(0\ V)} = 6$ nA) and D4 ($I_{(0\ V)} = 4$ nA), respectively. The total crosstalk of − 60 dB (0.10%), − 58 dB (0.12%), − 63 dB (0.07%), and − 60 dB (0.10%) was calculated using Eq. 3 for D1, D2, D3 and D4, respectively. Since each diode is individual from each other, the most important factors for low crosstalk values can be discussed as the constant length between diodes and the constant distance between the sample and the tip of the fiber optic cable in the measurement as summarized in Fig. 3 (c). Even the optical crosstalk effect is suppressed in our device structure, as the light source moves away from the diodes or the distance between the diodes gets closer, the possible crosstalk effect will increase due to the limitations in our measurement setup. For all the diodes, we observed similar trend but these small variations in optical crosstalk values can be caused by a trace amount of light which was randomly reflected back from the tip of the metallic casing of the fiber optic probe onto the surface of photoactive G/n-Si elements or due to the yield associated with graphene transfer process. After transfer process, there could be some local defects, cracks or wrinkles which result in unintentionally doping of graphene or some inhomogeneities at the G/n-Si interface. These mechanisms affect the optoelectronic characteristics of the graphene based photodetectors [17]. The total optical crosstalk value that we obtain in G/n-Si Schottky PDA with *common* graphene electrode was ~0.25% (−52 dB) where $I_{(0\ V)} = \sim 6.3$ nA and $I_{SC\ (0\ V)} = \sim 2.4$ μA. Here in, we calculated total optical crosstalk value as ~0.10% (−60 dB) for individual diodes. The reason for obtaining high optical crosstalk in PDA with *common* graphene electrode is that the least resistive path for the holes is the one through the graphene and not the one through the Si substrate. When compared to the device with *common* graphene electrode, the one with disconnected graphene electrodes the magnitude of the optical crosstalk between the diodes was found to be decreased by a factor of 150%. The comparison of optical crosstalk values for G/n-Si Schottky PDA with *common* and *separate* graphene electrode per array in detail can be found in Table 1. Despite above mentioned relatively high crosstalk values, our diode array showed extremely low crosstalk when compared with a 2D back-illuminated silicon vertical p-i-n PDA with 16 × 16 elements device with pixel pitch of 1 mm, gap size of 200 μm and absorption layer thickness of 50 μm where the obtained crosstalk is 10% (−20 dB) [27],

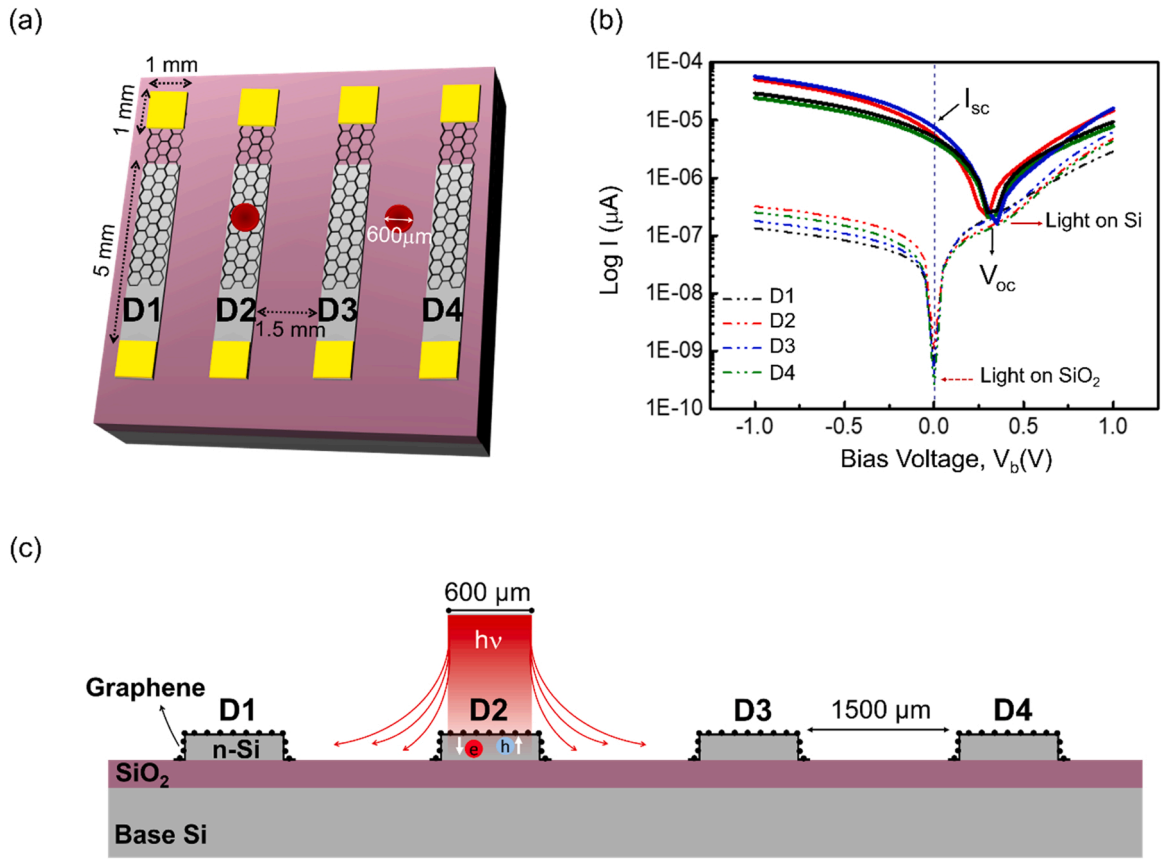

Fig. 3. Optical crosstalk measurement results of individual G/n-Si Schottky PDAs. (a) Local illumination on each diodes and illumination on SiO_2 regions located in between two neighboring diodes, (b) log(I)–V measurements acquired on diodes and on SiO_2 regions between them and (c) cross-sectional view of possible crosstalk elimination of our device structure. (The diodes were illuminated with 660 nm wavelength light having a power of 380 μW/mm^2.).

Table 1
Summary of the comparison of device performances of the diodes under 660 nm wavelength light at self-powered (0 V) operational mode. (Junction area 3 mm^2).

PDA Device Structure	ElementID	I_{dark} (nA)	Rmax (A/W)	D* (10^{12}) (Jones)	NEP (pW/Hz$^{1/2}$)	t_r (μs)	t_d (μs)	3-dB B_w (kHz)	OpticalCrosstalk (%)
Common Graphene Electrode[18]	D1	0.6	0.11	1.38	0.125	1.40	1.28	250	0.25
	D2	0.8	0.10	1.29	0.161	1.38	1.31	253	0.28
	D3	0.5	0.10	1.26	0.127	1.32	1.23	265	0.26
	D4	0.3	0.09	1.25	0.138	1.33	1.21	263	0.19
Separate Graphene Electrode (This Work)	D1	0.5	0.12	1.69	0.085	1.37	1.29	255	0.10
	D2	0.9	0.12	1.60	0.142	1.35	1.32	259	0.12
	D3	0.4	0.11	1.56	0.103	1.27	1.29	275	0.07
	D4	0.3	0.11	1.45	0.088	1.28	1.30	273	0.10

and the 4 channel InGaAs-based vertical p-i-n PDAs with 250 μm pitch which produced an optical crosstalk of − 35 dB (1.77%) [7]. Here, the determination of pixel pitch is essential because as the distance between electrodes were increased, the total crosstalk decreases for all devices in array. However, larger electrode distances cause the decrement in the speed of the device. As seen in the log(I)–V plots (Fig. 3(b)), all diodes exhibited a clear photovoltaic activity with measurable I_{SC} under light illumination. The shift of the minimum current seen at forward bias range (e.g., $V_b > 0.25$ V) corresponds to the open circuit voltage (V_{OC}) and is consistent with self-powered G/n-Si photodiodes operating in the self-powered mode [28]. It is well-known that, when G/n-Si heterojunction is subject to light illumination, the incident photons pass through the graphene and penetrate into the n-Si substrate to create e-h pairs in the depletion region (x_d). In the case of zero bias regime, the x_d is calculated between optically transparent graphene and ~10 μm thick n-Si substrate as 1 μm for a built-in potential (V_{bi}) of 0.7 V and a nominal donor doping concentration (N_d) of $\sim 2 \times 10^{15}$ cm^{-3}. Owing to the effective built-in electric field at the interface, measurable photocurrent is generated even at zero-bias. The absorption layer thickness has the most profound effect on the total crosstalk. There is a direct proportion between the absorption layer thickness and the crosstalk, because the probability of e-h diffusion to adjacent electrode pair is less for thin absorption thickness when compared with thicker one. For a thicker absorption layer, e-h can be generated deeper within the substrate and they are prone to diffuse to the neighbor electrodes hence increasing the total crosstalk. For instance, the substrate thickness is very critic for Ge-based ILPP arrays with an absorption thickness of 3 μm that show relatively high crosstalk of − 21 dB (8.9%) [5]. Here, the absorption (depletion) layer thickness in our devices is limited with x_d (1 μm) in self-powered mode. This also supports to gain extremely low crosstalk between individual diodes in the array even the effects of reflected light on the measured current are ignored. To summarize, we suppressed the effect of optical crosstalk in our device structure as in the following manner; (i) using n-Si substrate with a similar doping level of graphene

(unintentionally p-type doped with an intrinsic hole carrier concentration of about 10^{13} cm^{-2}), (ii) aligning the array geometry including the photodiode size and pitch of the detector array on SOI substrate and (iii) arranging the absorption layer as ~1 μm in zero-bias condition. The narrower depletion region minimizes the crosstalk effect compared to their counterparts working with external bias. Since the size of our devices is in the range of few millimeters (i.e., the distance between the diodes), the resolution is limited by the size of the LED spot. Indeed, the resolution of each element in PDA could easily be further improved by using a focused laser beam.

In order to determine the zero-bias (V_b = 0 V) spectral responsivity (R) of each element in the PDA, we conducted wavelength-resolved photocurrent spectroscopy measurements under illumination of light in the spectral range between 400 and 1050 nm. Here, R is defined as the ratio of generated photocurrent to the incident light power (P) at a certain wavelength. The maximum R of the diodes were observed as ~0.12 AW^{-1} at a peak wavelength of 660 nm and exhibited a decrement towards a cutoff wavelength of 1050 nm due to the band edge of n-Si substrate (Fig. 4(a)). The spectral responsivity of diodes exhibits two maxima located at around 660 nm and 780 nm wavelengths and decays earlier for the wavelengths above 780 nm. As we explain in our previous work [18], this phenomena can be understood by the contribution of the drift and diffusion currents, penetration depth of light and reduced absorption coefficient of Si layer on SOI structure when compared with bulk Si substrate. Besides, the BOX and Si handle layer make ineffective the remaining light power for photoresponse gain in SOI structure [26]. The active Si layer forms an optical microcavity for the G/n-Si Schottky PDA devices and causes an oscillating wavelength dependent responsivity. This mechanism is a result of constructive and destructive interference effects by favor of multiple reflections occurred between SOI interfaces.

Taking into account the R_{max} values read at 660 nm wavelength, we also calculated the specific detectivity (D*) and noise equivalent power (NEP) parameters of each active element in the array. Here, D* is defined as the weakest level of light detected by a photodiode having a junction area of 1 cm^2 and is determined by [17],

$$D^* = \frac{A^{1/2}R}{\sqrt{2qI_d}} \tag{5}$$

and NEP is the incident power required to obtain a signal-to-noise ratio of 1 at a bandwidth of 1 Hz and is calculated by [14,17],

$$NEP = \frac{A^{1/2}}{D^*} \tag{6}$$

D* and NEP of our samples were calculated using Eqs.5 and 6, respectively and the obtained results were displayed as a function of wavelength in Fig. 4(b) and (c), respectively. In agreement with the corresponding R_{max} = ~0.1 AW^{-1} with a junction area of 3 mm^2, the average D* and minimum NEP values were calculated at 660 nm peak wavelength. With D* = ~1.57 × 10^{12} Jones and NEP = ~0.121 pW/$Hz^{-1/2}$, each individual diodes showed similar light sensitivity among diodes with *common* graphene electrode [18] and these results are in good agreement with those of both single pixel G/Si PD on SOI [26] and G/Si PD on bulk Si substrates [17].

The response speed of the diodes in the PDA were carried out with one-cycle switching on/off within 0.08 ms using time-dependent photocurrent spectroscopy measurements. In the experiments, rise time (t_r) and decay time (t_d) of each individual element in the array were determined from single pulse response measurements taken under 660 nm wavelength light pulses with a frequency of 1 kHz. The measurements were done with the same manner in Ref [18]. Here t_r is defined as the range that the photocurrent rises from 10% to 90% of the peak amplitude output on the leading edge of the pulse and t_d is defined likewise. The measurements revealed that all the elements showed great capability to respond high-frequency pulsed light and on/off switching

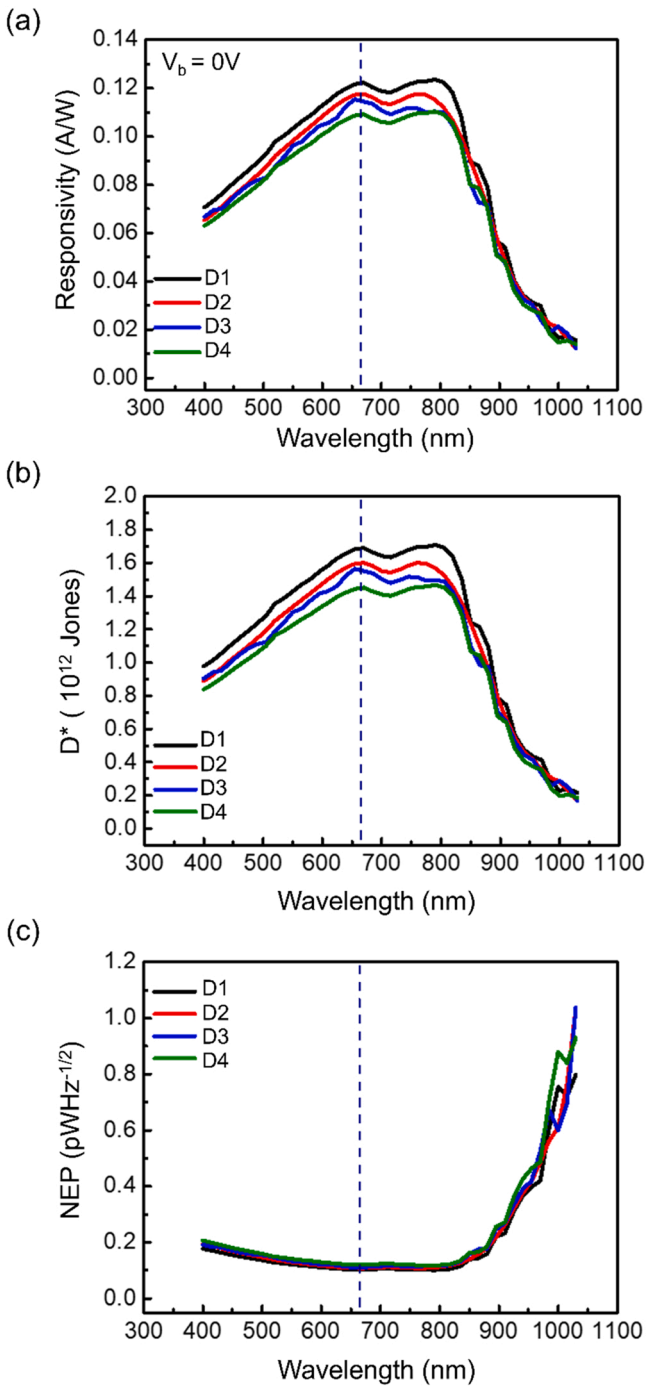

Fig. 4. (a) The spectral responsivity, (b) D* and (c) NEP of the fabricated individual diodes as a function of wavelength.

stability. The single pulse response measurement was done to extract the respond speed of each individual diodes with *separate* graphene electrode as shown Fig. 5(a-d). Considering the measurements taken on each elements, the average t_r and t_d were determined as ~1.32 μs and ~1.30 μs respectively. Using the 3-dB bandwidth (B_w) relation $B_w = 0.35/t_r$, the average 3-dB B_w of the diodes was calculated as ~266 kHz, respectively. For convenience, all the obtained performance parameters of each diode in the PDA device structures are listed and compared with our previous study and among themselves in Table 1 in detail. In addition, we also compared the device performance parameters of our device with previously reported graphene/Si based photodetectors fabricated on SOI structure in Table 2.

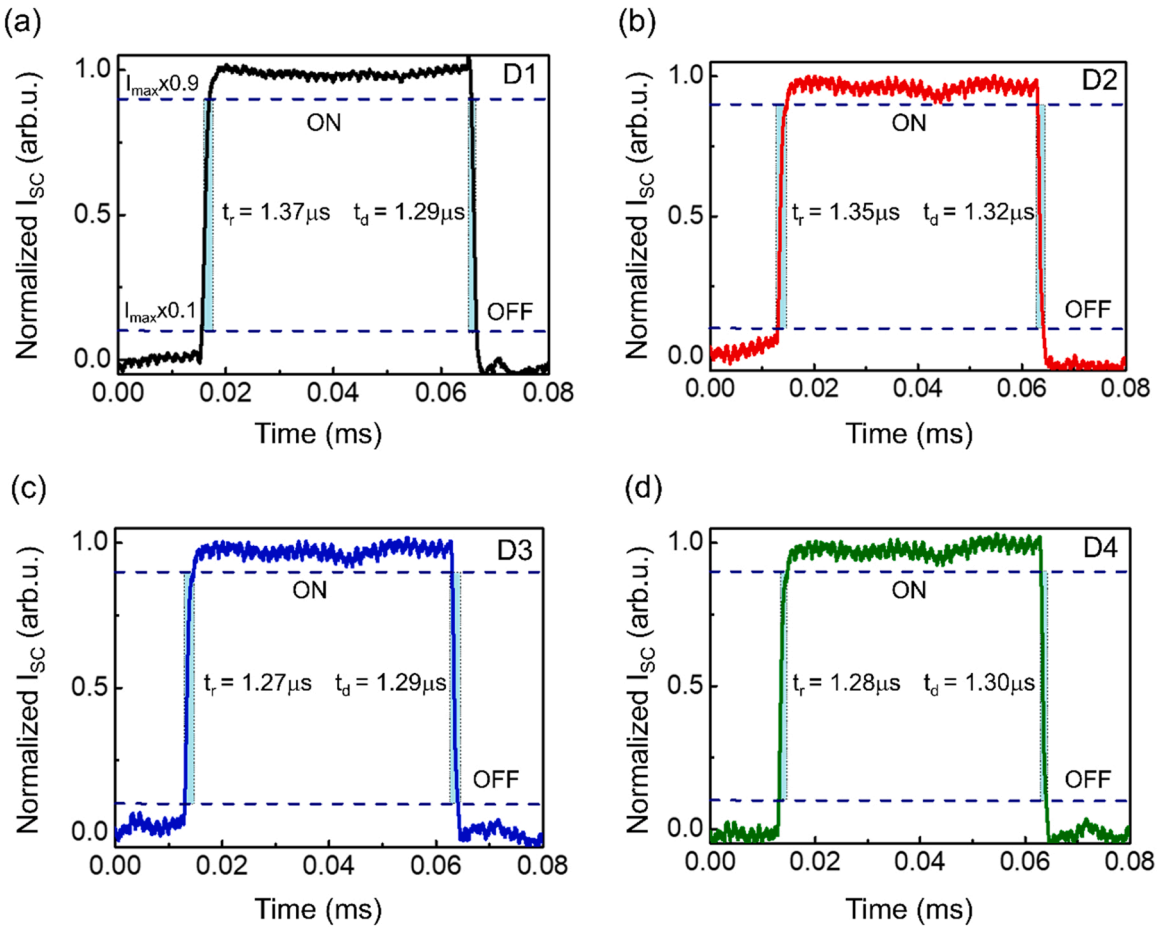

Fig. 5. The one cycle time-resolved photocurrent spectrum of an individual diodes under 660 nm wavelength light with 1 kHz switching frequency at zero-bias voltage; depending on the element name (a) D1, (b) D2, (c) D3 and (d) D4, respectively. The measured photocurrents were normalized with the maximum values.

Table 2
Comparison of the photoresponse properties of our device with previous reported graphene/Si photodetectors on SOI.

Types of Devices	Junction Area	Responsivity	Detectivity	Rise/Fall Time	Refs
Graphene–silicon-on Insulator	16 mm^2	0.26 A/W ($V_b = -2$ V; $\lambda = 635$ nm)	7.83×10^{10} Jones	~10 ns/ 20–70 ns	[26]
Graphene/silicon-on insulator in conductor mode	-	10^{17} A/W ($V_b = -30$ V; $\lambda = 532$ nm)	1.46×10^{13} Jones	90 μs/-	[29]
3D-graphene/SOI	-	27.4 A/W ($V_b = -0.5$ V; $\lambda = 1550$ nm)	1.37×10^{11} Jones	212 μs/ 242 μs	[30]
4-Element G/n-Si Schottky PDA with *separate* graphene electrode	3 mm^2	0.12 A/W ($V_b = 0$ V; $\lambda = 660$ nm)	1.57×10^{12} Jones	~1.32 μs/ ~1.30 μs	Our work

4. Conclusion

To conclude, the optoelectronic characteristics of individual G/n-Si based Schottky linear PDA on a conventional SOI substrate in terms of their spectral response, specific detectivity, noise equivalent power and response speed under self-powered condition and the suppression of the optical crosstalk encountered between each element was analyzed and examined. Individual monolayer graphene was utilized as optically transparent cathode electrode on arrayed 4-element n-Si fabricated on a single SOI substrate. All devices exhibited strong rectification behavior and have low leakage current in parallel with high detectivity, low noise and fast operation speed. We also revealed that separated G/n-Si diodes on a SOI operate independently from each other with an extremely low optical crosstalk. This study guided that the devices with *common* graphene electrode showed considerable suppression in terms of magnitude optical crosstalk compared to InGaAs, Si and Ge based p-i-n PDA counterparts. Conversely, the magnitude of optical crosstalk measured for devices with *separate* graphene electrode is even better than *common* electrode one which requires fewer lithography steps in fabrication route.

Declaration of Competing Interest

The authors declare that they have no known competing financial interests or personal relationships that could have appeared to influence the work reported in this paper.

Data Availability

No data was used for the research described in the article.

Acknowledgements

The authors would like to thank the researchers in Center for Materials Research of İzmir Institute of Technology (İYTE MAM) and Ermaksan Optoelectronic R&D Center in Turkey for their support in device fabrication processes. This work is supported within the scope of the scientific research project as a part of the Project No. BAP113 which was accepted by the Yaşar University Project Evaluation Commission (PEC).

References

[1] W. Gao, T. Ohnuma, H. Satoh, H. Shimizu, S. Kiyono, A precision angle sensor using a multi-cell photodiode array, CIRP Ann. 53 (2004) 425–428.
[2] S.G. Chamberlain, Photosensitivity and scanning of silicon image detector arrays, IEEE J. Solid-State Circuits 4 (1969) 333–342.
[3] Y. Talmi, R. Simpson, Self-scanned photodiode array: a multichannel spectrometric detector, Appl. Opt. 19 (1980) 1401–1414.
[4] M.-L. Hsia, Z.M. Liu, C.N. Chan, O.T.-C. Chen, Crosstalk effects of avalanche CMOS photodiodes, IEEE Sens. J. (2011) 1689–1692.
[5] P. Menon, B. Bais, A.A.M. Jhi, S. Shaari, Optical crosstalk in interdigitated lateral PIN photodiodes, Optoelectron. Adv. Mater. Rapid Commun. 6 (2012) 535–538.
[6] I. Rech, A. Ingargiola, R. Spinelli, I. Labanca, S. Marangoni, M. Ghioni, et al., Optical crosstalk in single photon avalanche diode arrays: a new complete model, Opt. Express 16 (2008) 8381–8394.
[7] T. Shirai, M. Minamino, T. Higuchi, M. Iwase, Low cross-talk 4ch PD array module assembled in plastic package for signal monitoring in DWDM system, Optical Fiber Communication Conference, Optica Publishing Group, (2001) p. WDD73.
[8] D. Dao, K. Nakamura, T. Bui, S. Sugiyama, SOI-based nanoelectrospray emitter tips for mass spectrometry: a coupled MEMS and microfluidic design, Adv., Nat. Sci. Nanosci. Nanotechnol. 1 (2010), 013001.
[9] D. Periyanagounder, P. Gnanasekar, P. Varadhan, J.-H. He, J. Kulandaivel, High performance, self-powered photodetectors based on a graphene/silicon Schottky, Junction Diode, J. Mater. Chem. C. 6 (2018) 9545–9551.
[10] J. Huang, Z. Zhong, Z. Jiang, F. Gao, Y. Zhang, F. Liu, et al., High-performance graphene/n-Si hybrid photodetector toward self-driven optical communications, Appl. Phys. Lett. 119 (2021), 263506.
[11] P. Lv, X. Zhang, X. Zhang, W. Deng, J. Jie, High-sensitivity and fast-response graphene/crystalline silicon Schottky junction-based near-IR photodetectors, IEEE Electron Device Lett. 34 (2013) 1337–1339.
[12] C.-C. Chen, M. Aykol, C.-C. Chang, A. Levi, S.B. Cronin, Graphene-silicon Schottky diodes, Nano Lett. 11 (2011) 1863–1867.
[13] T. Yu, F. Wang, Y. Xu, L. Ma, X. Pi, D. Yang, Graphene coupled with silicon quantum dots for high-performance bulk-silicon-based Schottky-junction photodetectors, Adv. Mater. 28 (2016) 4912–4919.
[14] S. Tongay, M. Lemaitre, X. Miao, B. Gila, B. Appleton, A. Hebard, Rectification at graphene-semiconductor interfaces: zero-gap semiconductor-based diodes, Phys. Rev. X. 2 (2012), 011002.
[15] H. Selvi, N. Unsuree, E. Whittaker, M.P. Halsall, E.W. Hill, A. Thomas, et al., Towards substrate engineering of graphene–silicon Schottky diode photodetectors, Nanoscale 10 (2018) 3399–3409.
[16] Y. Song, X. Li, C. Mackin, X. Zhang, W. Fang, T. Palacios, et al., Role of interfacial oxide in high-efficiency graphene–silicon Schottky barrier solar cells, Nano Lett. 15 (2015) 2104–2110.
[17] M. Fidan, Ö. Ünverdi, C. Çelebi, Junction area dependent performance of graphene/silicon based self-powered Schottky photodiodes, Sens. Actuator A Phys. (2021), 112829.
[18] A. Yanilmaz, M. Fidan, O. Unverdi, C. Çelebi, Graphene/SOI-based self-powered Schottky barrier photodiode array, Appl. Phys. Lett. 121 (2022), 011105.
[19] Y. Xu, A. Ali, K. Shehzad, N. Meng, M. Xu, Y. Zhang, et al., Solvent-based soft-patterning of graphene lateral heterostructures for broadband high-speed metal–semiconductor–metal photodetectors, Adv. Mater. Technol. 2 (2017) 1600241.
[20] A. Grillo, Z. Peng, A. Pelella, A. Di Bartolomeo, C. Casiraghi, Etch and print: graphene-based diodes for silicon technology, ACS Nano (2022).
[21] S.C. Baker-Finch, K.R. McIntosh, One-dimensional photogeneration profiles in silicon solar cells with pyramidal texture, Prog. Photovolt. 20 (2012) 51–61.
[22] N. Şahan, M. Fidan, C. Çelebi, Adsorbate-induced enhancement of the spectral response in graphene/silicon-based Schottky barrier photodetectors, Appl. Phys. A 126 (2020) 1–6.
[23] J. Park, A. Reina, R. Saito, J. Kong, G. Dresselhaus, M. Dresselhaus, G′ band Raman spectra of single, double and triple layer graphene, Carbon 47 (2009) 1303–1310.
[24] S. Sze, Physics of semiconductor devices 2nd edition, Microelectron. J. (1981).
[25] S. Cheung, N. Cheung, Extraction of Schottky diode parameters from forward current-voltage characteristics, Appl. Phys. Lett. 49 (1986) 85–87.
[26] H. Selvi, E.W. Hill, P. Parkinson, T.J. Echtermeyer, Graphene–silicon-on-insulator (GSOI) Schottky diode photodetectors, Nanoscale 10 (2018) 18926–18935.
[27] I. Goushcha, B. Tabbert, A.O. Goushcha, Optical and electrical crosstalk in pin photodiode array for medical imaging applications, IEEE Nuc. Sci. Conf. R., (2007), 4348–4353.
[28] A. Di Bartolomeo, Graphene Schottky diodes: an experimental review of the rectifying graphene/semiconductor heterojunction, Phys. Rep. 606 (2016) 1–58.
[29] H. Jiang, C. Nie, J. Fu, L. Tang, J. Shen, F. Sun, et al., Ultrasensitive and fast photoresponse in graphene/silicon-on-insulator hybrid structure by manipulating the photogating effect, Nanophotonics 9 (2020) 3663–3672.
[30] Z. He, G. Zhang, S. Zhang, X. Feng, Z. Liu, G. Wang, et al., Resonant nanocavity-enhanced graphene photodetectors on reflecting silicon-on-insulator wafers, Appl. Phys. Lett. 119 (2021), 232104.

Alper Yanilmaz received his MSc degree in Materials Science and Engineering at İzmir Institute of Technology (IZTECH). He is pursuing for his Ph.D. under the supervision of Prof. Dr. Cem Çelebi at the Quantum Device Laboratory (QDL) in Physics department of the same institute. His main research interests include Graphene synthesis and Graphene/Semiconductor heterojunction devices.

Özhan Ünverdi received his Ph.D. in 2005 from Physics Department of Loughborough University in UK. He is currently working as Assistant Professor in Electric-Electronics Engineering Department of Yaşar University. His main research areas are low-dimensional systems, tribology in nano-scale and scanning probe microscopy.

Cem Çelebi received his Ph.D. in 2009 from Applied Physics Department of Eindhoven University of Technology in the Netherlands. He is currently working as Professor in the Physics Department of IZTECH. He is the principal investigator and group leader of Quantum Device Laboratory at IZTECH. For further information please visit http://qdl.iyte.edu.tr/.